System identification of photosensitiser uptake kinetics in photodynamic therapy

Thierry Bastogne, Loraine Tirand, Denise Bechet, Muriel Barberi-Heyob, Alain Richard

System identification of photosensitiser uptake kinetics in photodynamic therapy

T. Bastogne[1], L. Tirand[2], D. Bechet[2], M. Barberi-Heyob[2], A. Richard[1]
[1] Centre de Recherche en Automatique de Nancy, CRAN
Nancy-Université, CNRS UMR 7039
Vandœuvre-lès-Nancy Cedex, France
Phone: (33) 3 83 68 44 73 - Fax: (33) 3 83 68 44 62
thierry.bastogne@cran.uhp-nancy.fr
[2] Centre de Recherche en Automatique de Nancy (CRAN)
Nancy - Université, CNRS UMR 7039,
Centre Alexis Vautrin, Centre de Lutte contre le Cancer
Brabois, Av. de Bourgogne, 54511 Vandœuvre-ls-Nancy Cedex, France

July 30, 2007

Abstract

This study draws the interest of system identification to the experimental modelling of *in vitro* uptake kinetics of photosensitising agents (PS) into cancer cells. The proposed identification methodology must be usable and valid for every PS. Therefore, three PSs characterized by opposing chemical and biological properties have been selected: (1) PC: a second generation photosensitising agent conjugated *via* a spacer to a VEGF receptor-specific heptapeptide, (2) Ce6: Chlorin e6, and (3) TPP: TetraPhenylPorphyrin. Experiments have been carried out with two rates (2% and 9%) of foetal bovin serum in the culture medium and one cancer cell line $U87$ a human malignant glioma. Difficulties of such an application are triple: (i) lack of data, (ii) low signal-to-noise ratio and (iii) 'poor' stimulus signals. The proposed identification methodology deals with the design of experiments, the selection of a model structure, the estimation of the model parameters and the estimation of the parameter uncertainties. The photosensitiser uptake phenomenon is described by a first-order transfer function. Estimates of the time constant and the static gain provide quantitative information about the uptake rate and yield of the PS. The parameter uncertainty is described by confidence regions in parameters space. This representation is presented as an efficient way to discriminate the uptake characteristics of different photosensitisers. This representation also emphasizes the effects of some biological factors, such as the serum rate, on the uptake yield[1].

[1]Draft version of the article printed in Biomedical Signal Processing and Control

Keywords System identification, pharmacokinetics models, drug delivery, photodynamic therapy.

1 Introduction

Photodynamic therapy (PDT) (Moser (1998)) is an emerging therapy for displastic tissues such as cancers. This therapy involves selective uptake and retention of a photosensitive drug (photosensitiser, PS) in a tumour, followed by irradiation with light at an appropriate wavelength. Photosensitisers are photoactive compounds such as for instance porphyrins and chlorins. The activated photosensitiser is thought to produce singlet oxygen at high doses and thereby to initiate apoptotic and necrotic death of tumour. In current clinical practice, photodynamic therapy is carried out with prescribed drug doses and light doses as well as fixed drug-light intervals and illumination fluence rates. These doses are determined from a physical model, see *e.g.* (Patterson *et al.* (1990); Hetzel *et al.* (2005)), defined by $[R] = k_s \cdot b \cdot \epsilon \cdot I_\lambda \cdot T \cdot [P_i] \cdot \Phi \cdot f$ where: $[R]$ is a threshold concentration of oxidising events radicals that needs to occur in a sensitive location within a cancer cell to elicit the cascade toward cell death. I_λ is the irradiance on the tissue surface, T is the exposure time of treatment light and $[P_i]$ is the concentration of intracellular photosensitive drug. k_s is the backscatter factor due to reflected light from underlying tissue, b is a conversion factor, ϵ is the extinction coefficient of photosensitive drug, Φ is the quantum yield for conversion of activated drug to oxidising radicals, which usually depends on the oxygen concentration dissolved in the cells and f is the fraction of generated oxidising radicals, which attack sensitive cellular sites, while the fraction $(1-f)$ of the radicals attack lesser sites and have minor effect. Despite its current use in clinical applications, several polemical points can be addressed against this model.

- Firstly, the simplified physical model, previously given, implies a simple reciprocity of photosensitiser concentration and light. Nevertheless, several experiments have shown contradictory results (Moesta *et al.* (1995)). Moreover Potter *et al.* have shown that a reduction in photosensitiser concentration during treatment, *e.g.* PS photodegradation, is an important consideration (Potter (1986)).

- The term (Φ) is function of oxygenation but is usually a unknown factor during PDT (Dysart *et al.* (2005)).

- Sites of photodamage mainly depend on the location of the PS in the cell. Sites of action for singlet oxygen in PDT include mitochondria, endoplasmic reticulum, Golgi apparatus, lysosomes, DNA and lipid membranes (Henderson and Dougherty (1992)). Some of them are critical sites. Unfortunately, this physical model does not take into account the intracellular location of PS.

- Moreover, most of quantities, such as I_λ and $[P_i]$, are time dependent (Dysart *et al.* (2005)).

This paper focuses on the latter point and more precisely the intracellular uptake kinetics of PS, or in other terms, the rate of photosensitising molecules being incorporated and accumulated by living cancer cells according to incubation terms (Barberi-Heyob *et al.* (2004)). The delivery control of the photosensitising agent into the cancer cells is one of the major factors which directly affect the therapeutic efficiency of the photodynamic therapy (PDT) (Moser (1998); Bonnett (2000)). Many investigations have focused on the relationship between the molecular structure of PS and their extent of uptake by artificial membranes and cells. These have included porphyrins (Oenbrink *et al.* (1988)) and structurally related compounds, such as phtalocyanines (Margaron *et al.* (1996)), chlorines and pyropheophorbides (Henderson *et al.* (1997)). These studies concluded that the intracellular uptake could not be predicted from the chemical properties. The current knowledge about the uptake kinetics of PS into target cells is usually described by a few data points obtained during *in vitro* kinetics experiments. However, this class of non-parametric models is not very well suited to the analysis, prediction and design of the PS uptake phase during PDT. The FDA's[2] 2004 Critical Path Report proposed, among other solutions, the increased use of model-based approaches to drug development, including pharmacokinetic and pharmacodynamic (PK/PD) modeling.

The determination of a parametric model describing the uptake kinetics of photosensitising agents into living cells by extracting information from observations of input and output variables is a system identification problem (Ljung (1987); Walter and Pronzato (1997)). Several papers have been reported for the application of system identification techniques to pharmacokinetics modelling problems (Feng *et al.* (1996); Gomeni *et al.* (1988); Cobelli *et al.* (2000); Delforge *et al.* (2000); Sparacino *et al.* (2000); Audoly *et al.* (2001)). In particular, let us cite works of N. D. Evans et al. in (Evans *et al.* (2004, 2005)) in which a mathematical model for the *in vitro* kinetics of the anti-cancer agent topotecan is proposed. However, topotecan is not a photosensitiser and system identification issues met in this study mainly come from the difficulty to accurately measure the temporal evolution of the intracellular PS concentration. Indeed, in practice $[P_i](t)$ is measured by a spectrofluorimeter but the latter induces a photobleaching process of the PS. The term photobleaching refers to the process by which the chromophoric structure of the PS is degraded by absorbed light energy (Niedre *et al.* (2003)). As PS can be photobleached after light exposure, repeated experimentations for the same biological sample are not conceivable. In other terms, one biological sample with PS cannot be used for consecutive measurements of $[P_i]$. Collecting n_t data points of the kinetics then requires to repeat n_t times the same experiment (n_t biological samples) with identical initial conditions. To avoid the time consuming and the too high cost of such an experiment set up, n_t is generally kept small, *i.e.* $n_t \leq 10$. This limitation

[2]U.S. Food and Drug Administration

on n_t is also true for n_e the number of repeated kinetics experiments. The second difficulty is the low signal-to-noise ratio. The latter point is due to a great measurement variability when working on living cells which are very sensitive to external disturbances. This variability of measurements is increased by the fact that data points are extracted from different biological samples in order to avoid the PS photobleaching phenomenon. Thirdly, the choice of the stimulus signal is restricted to step signals which correspond to the amount of PS injected into the culture medium wells at time $t = 0$. Indeed, changing the concentration of the PS in a culture medium is not as simple as modifying the current or voltage of an electric actuator.

The system identification problem addressed in this paper deals with the parameter estimation of continuous-time models from a small set of non uniformly sampled data characterized by low signal-to-noise ratios. No identification study has been applied to the *in vitro* uptake kinetic responses of PS into living cancer cells yet. The main contributions of this paper are twofold: (1) to assess the applicability of a 'classical' system identification technique to *in vitro* uptake data of three different PSs and (2) to propose a new representation of the PS uptake characteristics based on the estimated model parameters. Each step of the system identification methodology is presented: the design of experiments, the selection of a model structure, the estimation of the model parameters, the estimation of the parameter uncertainties and a biological interpretation of the results.

2 PS uptake kinetics modeling

The measurement variable y of the intracellular PS concentration $[P_i]^*$ is the variable to explain while the administrated PS concentration $[P_a]$ is the input variable. The protein concentration (or serum rate) $[Se]$ and the PS type are regarded as two input factors which are kept constant during the experiments. In *in vitro* experimental conditions, the uptake phenomenon of PS into cancer cells can be described by a mass balance equation,

$$Q_{Pa}(t) = Q_{Pi}(t) + Q_{Px}(t). \tag{1}$$

where Q_E denotes the quantity (mol) of the specie $E \in \{Pa, Pi, Px\}$. Px is the extracellular PS and is not measured in this study. t is the time variable. Concentrations are given by $[P_a](t) = Q_{Pa}(t)/V$, $[P_x](t) = Q_{Px}(t)/V_x$, $[P_i](t) = Q_{Pi}(t)/V_i$, where V, V_x and V_i denote the global, extracellular and intracellular volumes. It is assumed that the measurement variable provided by the spectrofluorimeter is proportional to the intracellular PS concentration, *i.e.* $y(t) \propto [P_i](t)$. The input-output relationship between $y(t)$ and $[P_a](t)$ is described at each sampling time instant t_j by

$$y(t_j) = y_{\mathcal{M}}(t_j, \mathbf{p}, [P_a]) + e(t_j) \tag{2}$$

where $y_{\mathcal{M}}$ is the output variable of the model $\mathcal{M}(t, \mathbf{p}, [P_a])$. $\mathbf{p}$ is the parameter vector of the model and $e(t)$ corresponds to the output error. $\{e(t_j)\}_{j=1}^{n_t}$ is

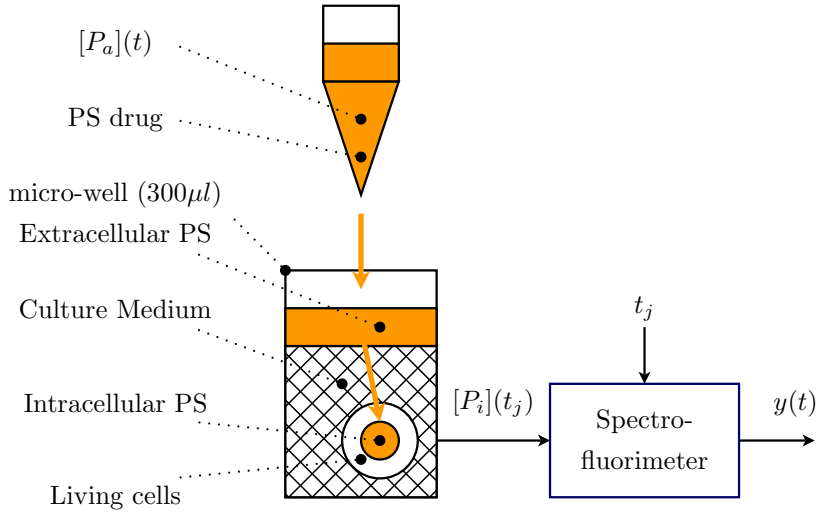

Figure 1: Material of the *in vitro* experiments, $[P_i]$ denotes the intracellular concentration of PS and y is the measurement of this concentration

assumed to be an independent and identically distributed sequence of gaussian variables $e(t_j) \sim \mathcal{N}(0, \sigma_e^2)$.

3 Design of experiments

3.1 Material and method

Fig.1 depicts the basic material used in *in vitro* experiments for studying the uptake kinetics of a photosensitising agent into living cells. Specific details about the preparation of the solutions were given in (Barberi-Heyob *et al.* (2004); Tirand *et al.* (2006)). Cancer cells are seeded in $250\mu L$ culture wells and are exposed at time $t_0 = 0$ to a step signal $[P_a](t) = 1\mu M$ of photosensitising drug. The output variable $y(t)$ is provided by a spectrofluorimeter at times $t_j \in \{1, 2, 4, 8, 18, 24\}$ $(hour)$. However, the spectrofluorimeter affects the biological state of the photosensitising drug through a photobleaching process. Each culture well then becomes unusable after measurement. Consequently, to measure the intracellular PS concentration at n_t different time instants, it is necessary to repeat the same experiment in n_t different culture wells, as illustrated in Fig.2. This problem would also occur if the measurement system was a high performance liquid chromatograph. The cancer cell line used for this application study is $U87$ a human malignant glioma.

The route by which a PS enters in cells depends on its physicochemical properties, *e.g.* its hydrophobicity/hydrophilicity; the type, number and arrangement of its charged groups; the presence of a central atom in the tetrapyr-

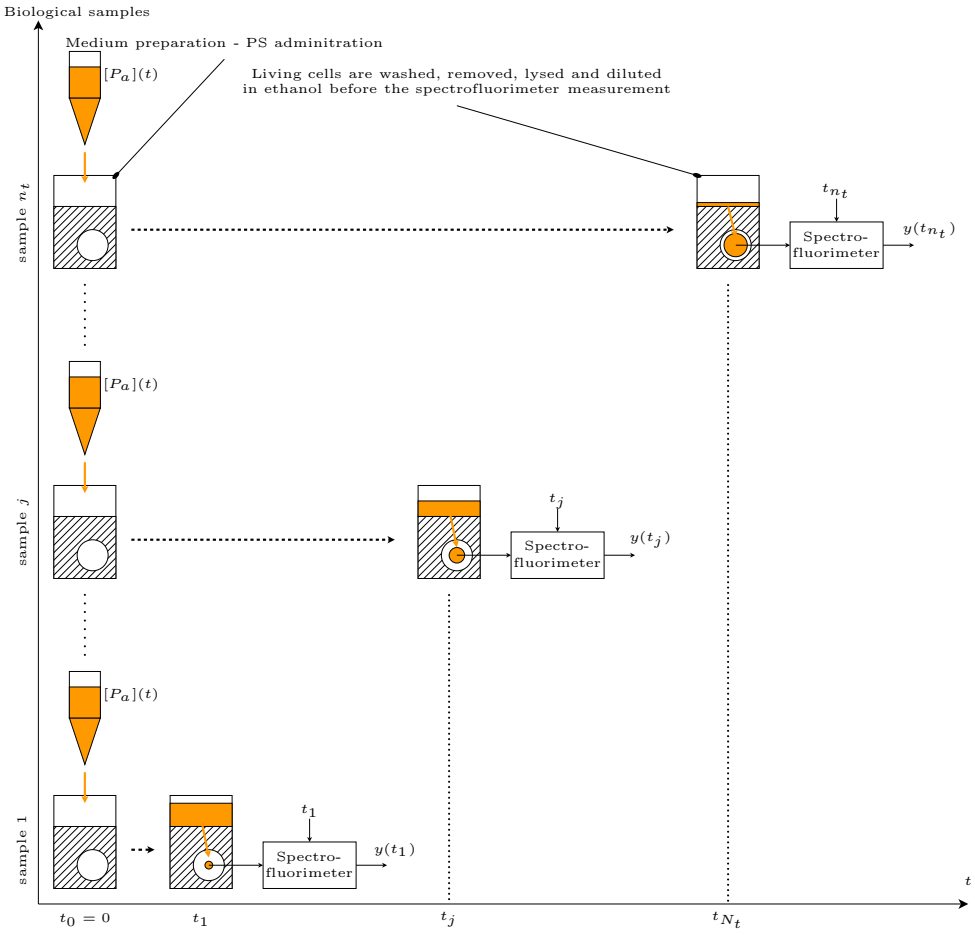

Figure 2: *in vitro* experimental set up

role structure; its aggregation state etc. For these reasons, the experiments were carried out for three different PSs: (1) PC: a second generation photosensitising agent (5-(4-carboxyphenyl)-10,15,20-triphenyl-chlorin, TPC) conjugated *via* a spacer (6-aminohexanoic acid, Ahx) to a VEGF (Vascular Endothelial Growth Factor) receptor-specific heptapeptide (TPC-Ahx-ATWLPPR) (Tirand *et al.* (2006)), (2) Ce6: Chlorin e6, and (3) TPP (TetraPhenylPorphyrin). We recently reported the synthesis and in vitro efficacy of a new peptide-conjugated PS (referred to hereafter as PC) having affinity for endothelial cells of the tumor neovasculature by targeting the Vascular Endothelial Growth Factor ($VEGF_{165}$) receptor neuropilin-1 (NRP-1), and not the type 2 VEGF receptor (VEGFR-2/KDR), as previously thought, through its peptidic moiety (Tirand *et al.* (2006)). PC displayed enhanced uptake and photodynamic properties in endothelial cells, compared to its non-conjugated counterpart TPC. The proposed identification methodology must be usable and valid for every PS. Therefore, we selected three PSs characterized by opposing chemical and biological properties. TPP and PC are hydrophobic PSs. Actually, the value of the octanol/ PBS distribution coefficient $\log D_{pH7.4}$ was equal to 2.6 ± 0.2, arguing for the hydrophobic character of PC (for details see (Tirand *et al.* (2007))). We previously used TPP as reference compound and demonstrated its hydrophobicity, in a first study describing the synthesis and the photodynamic activity in vitro of 4-carboxyphenylporphyrin-folic acid conjugates (Schneider *et al.* (2005)) and in a second one, studying the influence of structural modifications induced by symmetric or asymmetric glycoconjugation on photophysical properties and photosensitivity in vitro (Di Stasio *et al.* (2005)). Hydrophobicity/hydrophilicity properties of Ce6 were opposed compared to TPP and PC (Rosenkranz *et al.* (2000)).

The cell lines have been grown in two different culture medium: the first one is supplemented with 2% and the second one with 9% foetal bovin serum in order to assess the effect of the serum rate to the uptake kinetics. All these uptake kinetics experiments have been repeated three times.

3.2 Experimental data

Fig. 5 and 6 show six estimation data sets corresponding to the uptake kinetic responses of three PS (PC,Ce6,TPP) in two different culture medium ($[Se] = 2\%$ and $[Se] = 9\%$). Each uptake kinetic response is a step response obtained with $[P_a](t) = 1\mu M$. In these graphs, the solid line plot denotes the mean response over the three experiments. Each data point, described by a circle, a star or a triangle, is extracted from measurements performed during the three repeated experiments. Some outliers have been removed. Note that the variation between two samples measured at the same time can reach almost 100%, i.e. a signal-to-noise ratio estimated to $RSB \approx 0dB$.

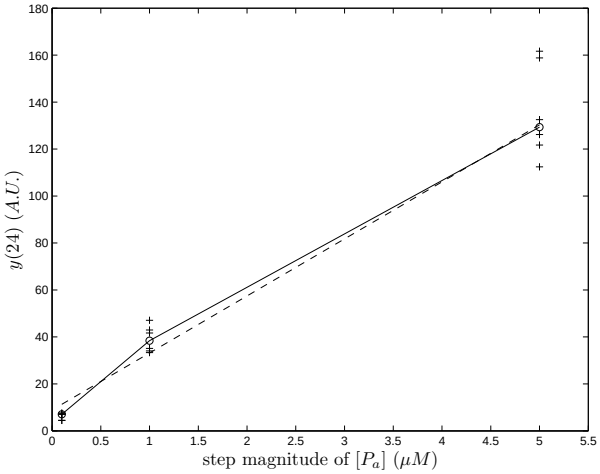

Figure 3: Test of linearity for PS=PC

3.3 Test of linearity

Three preliminary experiments have been carried out to measure at $t_j = 24\,h$ the intracellular PS concentration for three different values $(0.1, 1, 5\,\mu M)$ of the input step signal $[P_a]$. Results, presented in Fig. 3, exhibit a quasi-linear relationship between $y(t_j = 24)$ and $[P_a]$ over a range $[0.1 - 5]\mu M$ for one PS. Each experiment has been repeated six times; each outcome is described by a cross (+). The full line consists of the median values of the sextuplets. The dotted line, used as reference, is the least-squares line. It clearly appears that nonlinear model structures, *e.g.* Hammerstein-Wiener models, are not necessary in this case study. Similar results have been obtained for the two other PSs.

4 Selection of a model structure

This part deals with the determination of a parsimonious model structure ($\mathcal{M}(\mathbf{p})$) among a set $\mathbb{M}$ of candidate model structures. The dynamical behavior of $[P_i](t)$ can be explained by the two distinct biological phenomena: an uptake kinetics and a release kinetics of PS. In this paper, first-order model structures are used to described these two phases. Indeed, given the objectives of this study and the few number of available data points, this simplified model structure is suited to the experimental modeling of the PS uptake kinetics. Moreover, the model parameters, *i.e.* the time constant T and the static gain k are meaningful for the biologist. Indeed, they directly answer to two important questions asked by the biologist: (i) what is the PS uptake rate and (ii) what is the final yield of the PS uptake phenomenon, *i.e.* the ratio between the absorbed dose and the administrated dose of PS ? This first-order model structure is thus well suited to the purpose of this study. Two transfer functions $G_u(s)$ and $G_r(s)$ are proposed

for the description of the uptake and release kinetics respectively.

$$G_u(s) = \frac{k_u}{1+T_u s} \quad \text{and} \quad G_r(s) = \frac{k_r\, e^{-\tau_r s}}{1+T_r s}. \tag{3}$$

(k_u, k_r) and (T_u, T_r) denote the static gains and the time constants of the uptake and release kinetics. τ_r is the time-delay of the release phase and s is the Laplace variable. According to the PS, the release kinetics can sometimes be neglected in comparison with the magnitude of the uptake kinetics. Consequently, two model structures are candidate,

$$\mathcal{M}_1 : \quad y_{\mathcal{M}_1}(s) = G_u(s) \cdot [P_a](s), \tag{4}$$

if the release kinetics is negligible or

$$\mathcal{M}_2 : \quad y_{\mathcal{M}_2}(s) = (G_u(s) - G_r(s)) \cdot [P_a](s) \quad \text{otherwise.} \tag{5}$$

The selection between $\mathcal{M}_1$ and $\mathcal{M}_2$ can be performed by model choice criteria. A synoptic presentation of various available criteria of model structures in system identification, *e.g.* the Root Mean Squared Error (RMSE), the Akaike's Information Criterion (AIC), the Final Prediction Error (FPE), the F-test (or rather the χ^2 test), the Bayesian information criterion (BIC), are presented in (Söderström (1977); Walter and Pronzato (1997)). But for very small sample sizes, none of these criteria is recommended. In practice, when the ratio of the numbers of observations to parameters is lower than 40:1, it is better to use AICc (Burnham and Anderson (2002)) a variation of AIC defined by :

$$J_{AICc} = J_{AIC} + 2n_p(n_p+1)/(N-n_p-1), \tag{6}$$

with $n_p = \dim(\mathbf{p}_i)$, $i \in \{1,2\}$ and $J_{AIC} = 1/2 \cdot \ln(\hat{\sigma}^2_{e_i}) + 1/N \cdot \dim(\mathbf{p}_i)$. $N = n_t \cdot n_e$ and $\hat{\sigma}^2_{e_i}$ denotes the empirical estimate of the error variance, defined by

$$\hat{\sigma}^2_{e_i} = \frac{1}{N}\sum_{j=1}^{N} (y(t_j) - \hat{y}_{\mathcal{M}_i}(t_j, \mathbf{p}_i))^2, \tag{7}$$

over the n_e repeated experiments composed each of n_t data samples[3]. The model selection criterion is defined by :

$$\widehat{\mathcal{M}}(\hat{\mathbf{p}}) = \arg \min_{\mathcal{M}_i \in \mathbb{M}} \min_{\mathbf{p}_i \in \mathbb{P}_i} J_{AICc}(\mathcal{M}_i(\mathbf{p}_i)). \tag{8}$$

One rule of thumb says that the difference between the AICc value for two models is meaningful if this difference is greater than about 10, then the worse model can be neglected in the selection process, see (Burnham and Anderson (2002)).

[3] In theory, Eq. (7) is correct provided that the variance σ^2_e is estimated independently. Unfortunately in this application study, the number of data samples is too small to get an independent estimate of σ^2_e. As a consequence, the computation of $\hat{\sigma}^2_e$ is probably less accurate herein

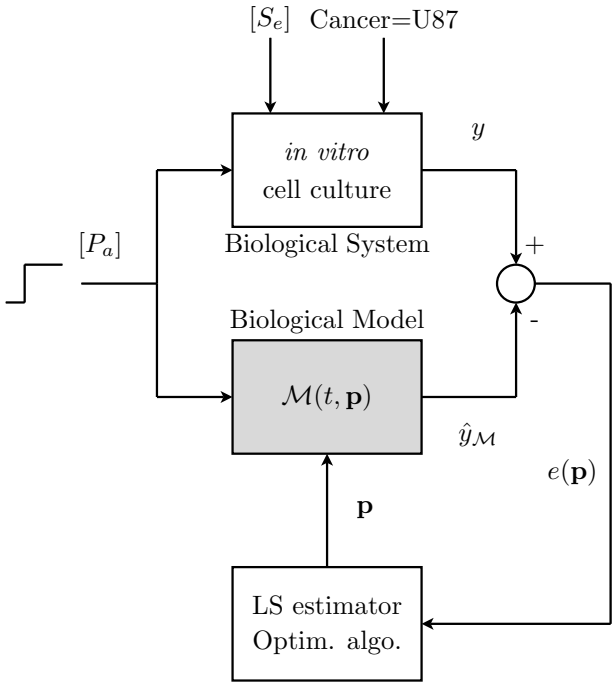

Figure 4: Output error method for a parallel model

For each model structure, $\hat{\mathbf{p}}_i$ is obtained by a non linear least squares estimator, as shown in Fig.4. Results of the model structure selection are gathered in Tab. 1. J denotes the output mean square error. Minimal values of criteria are indicated by bold typeface. According to J_{AICc}, the most parsimonious model structure is always $\mathcal{M}_1$. By examining more carefully the values of J and the estimated step responses presented in fig. 5(b) and 6(b), it clearly appears that the uptake-release model structure ($\mathcal{M}_2$) better fits the uptake responses of the Chlorin e6 than $\mathcal{M}_1$. This result implies that the release process is more significant with this PS than with the other ones.

Table 1: Model selection results

	J		J_{AICc}	
	$\mathcal{M}_1$	$\mathcal{M}_2$	$\mathcal{M}_1$	$\mathcal{M}_2$
PC-2	0.0769	**0.0672**	**-1.6992**	3.0103
Ce6-2	4.1023e-04	**2.6875e-04**	**-4.3109**	0.2515
TPP-2	**5.5964e-04**	5.6261e-04	**-4.1558**	0.6206
PC-9	**0.0676**	**0.0676**	**-1.7827**	3.0123
Ce6-9	6.4916e-05	**5.8003e-05**	**-5.2327**	-0.5153
TPP-9	**1.0398e-04**	1.0758e-04	**-4.9972**	-0.2068

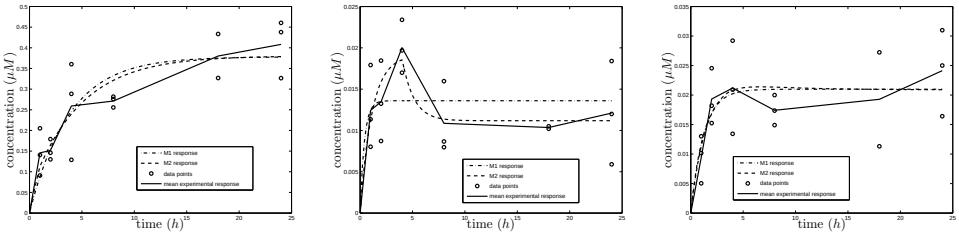

(a) PS=PC *(b)* PS=Ce6 *(c)* PS=TPP

Figure 5: Uptakes responses for $[S_e] = 2\%$, measured responses (solid line) and models responses (dotted lines)

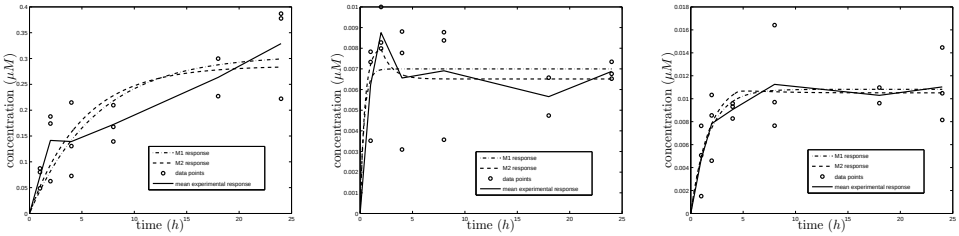

(a) PS=PC *(b)* PS=Ce6 *(c)* PS=TPP

Figure 6: Estimated responses for $[S_e] = 9\%$, measured responses (solid line) and models responses (dotted lines)

5 Parameter estimation

The parameter estimation relies on the output error method for a parallel model as shown in Fig. 4. The implementation of the least-squares estimator is based on a Levenberg Marquardt algorithm. Parameter estimates are given in table 2. Figures 5 and 6 compare the measured (mean values) and estimated step responses of $\mathcal{M}_1$ (dashdot (-.) plots) and $\mathcal{M}_2$ (dashed (–) plots) for the two values of $[S_e]$.

Table 2: Estimation results

	$[Se] = 2\%$		$[Se] = 9\%$	
	k_u	T_u	k_u	T_u
PC	0.3782	3.7845	0.3067	6.4516
Ce6	0.0136	0.4062	0.0070	0.3894
TPP	0.0210	1.2139	0.0108	1.7213

6 Model validation

Given the experimental conditions (lack of data and low signal-to-noise ratio), the model validation is an open problem. Firstly, the noise assumption (gaussian and i.i.d. stochastic process) cannot be checked. Indeed, the number of residual realizations ($n_e \cdot n_t = 18\,pts$) is too small to get a relevant histogram. Moreover, the measurement variability between two experiments (due in particular to the high sensitivity of living cells to external disturbances) is so high that any cross-validation test is not meaningful at all. In perspective, it would be interesting to assess recent alternative estimation approaches like the interval analysis Jaulin *et al.* (2001) or the Leave-out Sign-dominant Correlation Regions proposed by Campi and Weyer in Campi and Weyer (2006). Main advantages of such approaches is that they rely on less restrictive assumptions about the stochastic properties of the output error.

7 Parameter uncertainty

Because of the low signal-to-noise ratio, determining the optimal value of the parameters with respect to a chosen criterion is not enough. The relevance of the parameter analysis requires to evaluate the uncertainty associated with those estimates. Herein, parameters uncertainty is described by confidence regions, noted $\mathcal{R}^\alpha$, defined in Hamilton *et al.* (1982); Walter and Pronzato (1997) as follows:

$$\mathcal{R}^\alpha = \left\{ \mathbf{p} \in \mathbb{R}^{n_p} | \frac{\mathbf{e}^T(\mathbf{p})\Pi(\mathbf{p})\mathbf{e}(\mathbf{p})}{n_p \hat{\sigma}^2} \leq F_\alpha(n_p, N-1) \right\} \tag{9}$$

$\mathcal{R}^\alpha$ defines a $100(1-\alpha)\%$ confidence region for the parameters. $F_\alpha(n_1, n_2)$ denotes a Fisher-Snedecor distribution with n_1 and n_2 degrees of freedom. $\mathbf{e}(\mathbf{p}) = \mathbf{y} - \hat{\mathbf{y}}_\mathcal{M}(\mathbf{p})$ is the output error vector $\in \mathbb{R}^N$. $\mathbf{y}$ and $\hat{\mathbf{y}}_\mathcal{M}$ are defined by

$$\mathbf{y} = (y_1(t_1), \cdots, y_1(t_{nt}), \cdots, y_{n_e}(t_1), \cdots, y_{ne}(t_{nt})) \tag{10}$$

$$\hat{\mathbf{y}}_\mathcal{M} = (\hat{y}_{\mathcal{M},1}(t_1), \cdots, \hat{y}_{\mathcal{M},1}(t_{nt}), \cdots, \hat{y}_{\mathcal{M},n_e}(t_1), \cdots, \hat{y}_{\mathcal{M},ne}(t_{nt})) \tag{11}$$

where $y_k(t_j)$ denotes the j^{th} data sample collected during the k^{th} experiment ($k \in \{1, \cdots, n_e\}$). The orthogonal projection matrix $\Pi(\mathbf{p})$ is given by:

$$\Pi(\mathbf{p}) = S_{\hat{\mathbf{y}}_\mathcal{M}} (S^T_{\hat{\mathbf{y}}_\mathcal{M}} \cdot S_{\hat{\mathbf{y}}_\mathcal{M}})^{-1} S^T_{\hat{\mathbf{y}}_\mathcal{M}}, \tag{12}$$

where $S_{\hat{\mathbf{y}}_\mathcal{M}} = \partial \hat{\mathbf{y}}_\mathcal{M}(\mathbf{p}) / \partial \mathbf{p}^T$ is the sensitivity function (gradient) of the output model in respect with the parameter vector. The estimated noise variance[4] is

[4] For the same reasons than Eq. (7), the computation of $\hat{\sigma}^2$ is less accurate than theoretically expected since its independent estimation is not possible in this practical framework.

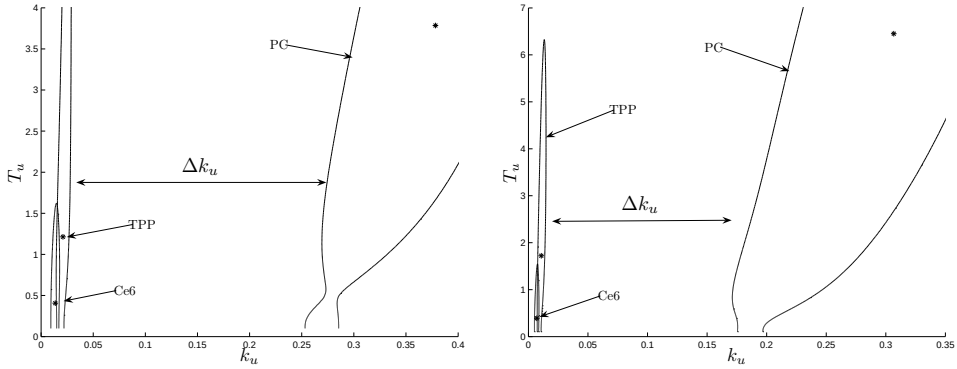

(a) $[S_e] = 2\%$ *(b)* $[S_e] = 9\%$

Figure 7: Locations of PSs in the $T_u - k_u$ parameter space

given by:

$$\hat{\sigma}^2 = \frac{1}{N-1} \sum_{j=1}^{n_t} \sum_{k=1}^{n_e} (y(t_{j,k}) - \bar{y}_j)^2$$
$$\bar{y}_j = \frac{1}{n_e} \sum_{k=1}^{n_e} y(t_{j,k}). \tag{13}$$

n_e refers to the number of repeated experiments. The 95% confidence regions of parameters for the three PS and for the two serum rates are presented in Fig. 7 and 8. The interest of 95% confidence regions is to allow a more robust comparative analysis (holding account of uncertainties) than a study only based on the parameter estimates.

8 Comparative study

8.1 Comparative study of PS

Fig. 7 shows the locations of confidence regions in the $T_u - k_u$ parameter space. Whatever the value of the serum rate, Fig. 7(a) and 7(b) show that comparatively to Ce6 and TPP, the confidence regions of PC are located towards the high values of k_u. More precisely, the uptake yield of PC is about 15 to 30 larger than the ones of Ce6 and TPP. This result is not surprising because PC is especially designed to target cancer cells like $U87$.

8.2 Comparative analysis of the serum effect

Figure 8 shows the effects of the serum rate on k_u and T_u. In Fig. 8(b) and 8(c), the increase of $[Se]$ causes the shift of confidence regions towards the low values

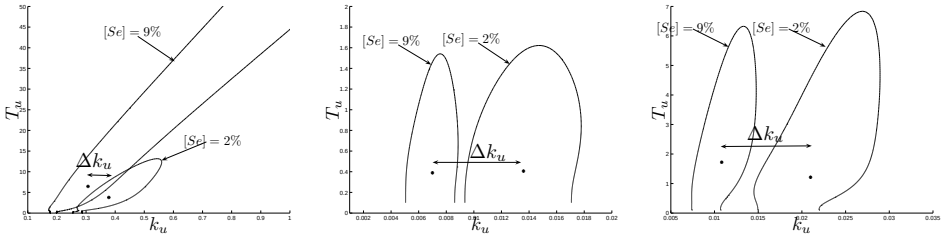

(a) PS=PC *(b)* PS=Ce6 *(c)* PS=TPP

Figure 8: Serum effect on the model parameters

of k_u. On the other hand, no change is observed about T_u (no vertical shift of confidence regions). The fall of k_u caused by the increase of $[Se]$ is also perceptible for PS in Fig. 8(a). A main difference between PC and the two other PSs concerns the extent of uncertainty for T_u. Indeed, a vertical shift and a dilation of the PS-confidence region is observed in Fig. 8(a). This result confirms that T_u is increasing with $[Se]$, particularly for PC. These results, obtained for three PSs, are in accordance with the results presented in (Bastogne *et al.* (2006)), in which an inversely proportional relationship between the static gain and the serum rate was identified for PS=Ce6 applied to another cancer cell line: HT29A4, a human colon cancer cell line.

One of the parameters widely influencing photophysical and pharmacological behaviour of PSs is their aggregation state. In aqueous media like culture media, most of the tetrapyrrolic PSs form dimers and higher micelle-like aggregates. Since more than twenty years, binding to proteins was believed to be an important factor for PSs cellular uptake (Hilf *et al.* (1983)). Actually, during interactions with proteins, a hydrophobic sensitizer dissociates from an aggregate and binds to protein molecules. Moreover, the type of protein-carrier governs the delivery of sensitizer to the tumor cells (Jori and Reddi (1993)).

9 Conclusion

This study draws the interest of system identification to the experimental modelling of *in vitro* uptake kinetics of photosensitising agents into cancer cells. Experiments have been carried out with three different photosensitisers (1) TPC-Ahx-ATWLPPR: a second generation photosensitising agent conjugated *via* a spacer to a VEGF receptor-specific heptapeptide, (2) Ce6: Chlorin e6, and (3) TPP (TetraPhenylPorphyrin), two rates (2% and 9%) of foetal bovin serum in the culture medium and one cancer cell line $U87$ a human malignant glioma. Difficulties of such an application are triple: (i) lack of data, (ii) low signal-to-noise ratio and (iii) 'poor' stimulus signals. The first two issues are mainly due to the measurement system, a spectrofluorimeter, which affects the biological state of the photosensitising drug through a photobleaching process. Unfortunately currently, there is no alternative way to measure the intracellular concentra-

tion of photosensitising agents in living cells. The system identification problem addressed in this paper concerns the parameter estimation of continuous-time models from a small set of non uniformly sampled data characterized by low signal-to-noise ratios. The proposed identification methodology deals with the design of experiments, the selection of a model structure, the estimation of the model parameters and the estimation of the parameter uncertainties. The photosensitiser uptake phenomenon is described by a first-order transfer function. Estimates of the time constants and the static gains provide quantitative information about the uptake rates and yields of the PSs respectively. The parameter uncertainty is described by confidence regions in parameters space. This representation is presented as an efficient and robust way to discriminate the uptake characteristics of different photosensitisers by holding account of uncertainties. In this application, this representation emphasizes the effects of the serum rate on the uptake yield. This application also stresses in these restricted experimental conditions that model validation is still an open problem. Future investigations should be oriented towards the development of small sample statistics and their application to pharmacokinetic and pharmacodynamic modelling.

References

Audoly, S., G. Bellu, L. D'Angio, M.P. Saccomani and C. Cobelli (2001). Global identifiability of nonlinear models of biological systems. *IEEE Trans. Biomed. Eng.* **48**, 55–65.

Barberi-Heyob, M., P.-O. Védrine, J.-L. Merlin, R. Millon, J. Abecassis, M.-F. Poupon and F. Guillemin (2004). Wild-type p53 gene transfer into mutated p53 HT29 cells improves sensitivity to photodynamic therapy via induction of apoptosis. *Int. J. Oncol.* (24), 951–958.

Bastogne, T., L. Tirand, M. Barberi-Heyob and A. Richard (2006). System identification of photosensitiser uptake kinetics in photodynamic therapy. In: *Proc of the 6th IFAC Symposium on Modelling and Control in Biomedical Systems (including Biological Systems)*. Reims, France.

Bonnett, R. (2000). *Chemical Aspects of Photodynamic Therapy*. Gordon and Breach Science Publishers.

Burnham, K. P. and D. R. Anderson (2002). *Model Selection and Multimodel Inference: a Practical Information-Theoretic Approach*. Springer-Verlag.

Campi, M. C. and E. Weyer (2006). Identification with finitely many data points: The LSCR approach. In: *Proc. of the 14th IFAC Symposium on System Identification (SYSID)*. Newcastle, Australia.

Cobelli, C., G. Toffolo and D. Foster (2000). *Tracer Kinetics in Biomedical Research: From Data to Model*. Kluwer Academic Publishers.

Delforge, J., A. Sirota and M. B. Mazoyer (2000). Identifiability analysis and parameter identificaion of an *in vivo* ligand-receptor model from PET data. *IEEE Trans. Biomed. Eng.* **37**(7), 653–661.

Di Stasio, B., C. Frochot, D. Dumas, P. Even, J. Zwier, A. Müller, J. Didelon, F. Guillemin, M. L. Viriot and M. Barberi-Heyob (2005). The 2-aminoglucosamide motif improves cellular uptake and photodynamic activity of tetraphenylporphyrin. *Eur. J. Med. Chem.* **40**, 1111–1122.

Dysart, J. S., G. Singh and M. Patterson (2005). Calculation of singlet oxygen dose from photosentitizer fluorescence and photobleaching during mTHPC photodynamic therapy of MLL cells. *Photochem. Photobiol.* (81), 196–205.

Evans, N. D., R. J. Errington, M. J. Chapman, P. J. Smith, M. J. Chappell and K. R. Godfrey (2005). Compartmental modelling of the uptake kinetics of the anti-cancer agent topotecan in human breast cancer cells. *International Journal of Adaptive Control and Signal Processing* **19**, 395–417.

Evans, N. D., R. J. Errington, M. Shelley, G. P. Feeney, M. J. Chapman, K. R. Godfrey, P. J. Smith and M. J. Chappell (2004). A mathematical model for the *in vitro* kinetics of the anti-cancer agent topotecan. *Mathematical Biosciences* **189**, 185–217.

Feng, D., S. C. Huang, Z. Wang and D. Ho (1996). An unbiased parametric imaging algorithm for non-uniformly sampled biomedical system parameter estimation. *IEEE Transactions on Medical Imaging* **15**(4), 512–518.

Gomeni, R., H. Piet-Lahanier and E. Walter (1988). Study of the pharmacokinetics of betaxolol using membership set estimation. *Biomed. Meas. Infor. Contr.* **2**(4), 207–211.

Hamilton, D. C., D. G. Watts and D. M. Bates (1982). Accounting for intrinsic nonlinearities in nonlinear regression parameter inference regions. *The Annals of Stat.* **10**, 386–393.

Henderson, B. W. and T. J. Dougherty (1992). How does photodynamic therapy work?. *Photochem. Photobiol.* **55**, 145–157.

Henderson, B. W., D. A. Bellnier DA, W. R. Greco, R. K. Sharma, R. K. Pandey, K. R. Weishaupt L. A. Vaughan and T. J. Dougherty. (1997). An *in vivo* quantitative structure-activity relationship for a congeneric series of pyropheophorbide derivatives as photosensitizers for photodynamic therapy. *Cancer Research* **57**, 4000–4007.

Hetzel, F. W., S. M. Brahmavar, Q. Chen, S. L. Jacques, M. S. Patterson, B. C. Wilson and T. C. Zhu (2005). Photodynamic therapy dosimetry. AAPM report No.88. American Association of Physicists in Medicine by Medical Physics Publishing.

Hilf, R., P. B. Leakey, S. J. Sollott and S. L. Gibson (1983). Photodynamic inactivation of R3230AC mammary carcinoma *in vitro* with hematoporphyrin derivative: effects of dose, time, and serum on uptake and phototoxicity.. *Photochem. Photobiol.* **37**, 633–42.

Jaulin, L., M. Kieffer, O. Didrit and E. Walter (2001). *Applied Interval Analysis*. Springer.

Jori, G. and E. Reddi (1993). The role of lipoproteins in the delivery of tumour-targeting photosensitizers. *Int. J. Biochem.* **25**, 1369–1375.

Ljung, L. (1987). *System Identification: Theory For The User*. Prentice Hall. Englewood Cliffs, NJ.

Margaron, P., H. Ali M.-J. Grégoire, V. Scasnar and J. E. van Lier (1996). Structure-photodynamic activity relationships of a series of substituted zinc phthalocyanines. *Photochem. Photobiol.* **63**, 217–223.

Moesta, K. T., W. R. Greco, S. O. Nurse-Finlay, J. C. Parsons and T. S. Mang (1995). Lack of reciprocity in drug and light dose dependence of photodynamic therapy of pancreatic adenocarcinoma *in vitro*. *Cancer Res.* **55**(14), 3078–3084.

Moser, J. G. (1998). *Photodynamic Tumor Therapy: 2nd and 3rd Generation*. Gordon & Breach Science Publishers.

Niedre, M. J., A. J. Secord, M. S. Patterson and B. C. Wilson (2003). *In vivo* tests of the validity of singlet oxygen luminescence measurements as a dose metric in photodynamic therapy. *Cancer Research* **63**, 7986–7994.

Oenbrink, G., P. Jurgenlimke and D. Gabel (1988). Accumulation of porphyrins in cells: influence of hydrophobicity aggregation and protein binding. *Photochem. Photobiol.* **48**, 451–456.

Patterson, M.S., B.C. Wilson and R. Graff (1990). *In vivo* tests of the concept of photodynamic threshold dose in normal rat liver photosensitized by aluminum chlorosulphonated phthalocyanine. *Photochem. Photobiol.* **51**, 343–349.

Potter, W. R. (1986). The theory of photodynamic therapy dosimetry: consequences of photodestruction of sensitizer. *Lasers Med.* **712**, 124–129.

Rosenkranz, A. A., D. A. Jans and A. S. Sobolev (2000). Targeted intracellular delivery of photosensitizers to enhance photodynamic efficiency.. *Immunol. Cell. Biol.* **78**, 452–464.

Schneider, R., F. Schmitt, C. Frochot, Y. Fort, N. Lourette, F. Guillemin, J.-F. Müller and M. Barberi-Heyob (2005). Design, synthesis, and biological evaluation of folic acid targeted tetraphenylporphyrin as novel photosensitizers for selective photodynamic therapy. *Bioorg. Med. Chem.* **13**, 2799–2808.

Söderström, T. (1977). On model structure testing in system identification. *Int. J. Control* **26**, 1–18.

Sparacino, G., C. Tombolato and C. Cobelli (2000). Maximum-likelihood versus maximum a posteriori parameter estimation of physiological system models: the C-peptide impulse response case study. *IEEE Trans. Biomed. Eng.* **47**(6), 801–811.

Tirand, L., C. Frochot, R. Vanderesse, N. Thomas, E. Trinquet, S. Pinel, M.-L. Viriot, F. Guillemin and M. Barberi-Heyob (2006). A peptide competing with $VEGF_{165}$ binding on neuropilin-1 mediates targeting of a chlorin-type photosensitizer and potentiates its photodynamic activity in human endothelial cells. *Journal of Controlled Release* **111**, 153–164.

Tirand, L., N. Thomas, M. Dodeller, D. Dumas D, C. Frochot, F. Guillemin and M. Barberi-Heyob (2007). Metabolic profile of a peptide-conjugated chlorin-type photosensitizer targeting neuropilin-1: an *in vivo* and *in vitro* study. *Drug Metab. Dispos.* **35**, 806–813.

Walter, E. and L. Pronzato (1997). *Identification of Parametric Models from experimental data*. Springer-Verlag, Masson.